The Veterinary Journal 190 (2011) 154–159

Contents lists available at ScienceDirect

The Veterinary Journal

journal homepage: www.elsevier.com/locate/tvjl

Ultrasonographic assessment of maternal cardiac function and peripheral circulation during normal gestation in dogs

Paula G. Blanco [a,*], Mariana Tórtora [a], Raúl Rodríguez [a], Daniel O. Arias [a], Cristina Gobello [b]

[a] Cardiology Service, Faculty of Veterinary Sciences, National University of La Plata (FVS-NULP), 60 y 118, La Plata 1900, Argentina
[b] Laboratory of Reproductive Physiology, FVS-NULP, La Plata, Argentina

ARTICLE INFO

Article history:
Accepted 30 August 2010

Keywords:
Doppler ultrasound
Echocardiography
Pregnancy
Shortening fraction
Dog

ABSTRACT

The aim of this study was to describe changes in cardiac morphology, systolic function and some peripheral hemodynamic parameters during normal pregnancy in dogs. Twenty healthy bitches, 10 pregnant (PG) and 10 non-pregnant controls (CG), were evaluated every 10 days using echocardiography from day 0 of the estrus cycle to parturition or to day 65 for the PG and CG groups, respectively. Systolic blood pressure (SBP) and uterine artery resistance index (RI) were also assessed.

Throughout the study, the shortening fraction and cardiac output increased up to 30% vs. 5% ($P < 0.01$) and 45% vs. 2% ($P < 0.01$) in the PG and CG groups, respectively. In contrast, SBP and RI diminished up to 20% vs. 1% ($P < 0.01$) and 29% vs. 0% ($P < 0.01$) in the PG and CG groups, respectively. In conclusion, a decrease in afterload, an increase in cardiac output and cardiac hypertrophy appear to be the result of the hemodynamic modifications occurring during pregnancy in dogs.

Introduction

The hemodynamic changes occurring during pregnancy have been described in mice and humans (Eghbali et al., 2005; Valensise et al., 2000; Blanco et al., 2008). Cardiovascular adaptation during gestation guarantees appropriate development of the fetuses. M-mode, 2D and Doppler echocardiography have been widely used in human medicine to assess systolic function and morphological left ventricular serial changes throughout pregnancy (Valensise et al., 2000; Kametas et al., 2001a).

In women, volume overload during pregnancy induces cardiac hypertrophy with corresponding augmentation of left ventricular (LV) mass and increased cardiac output (CO) (Kametas et al., 2001a; Desai et al., 2004). Ejection-phase indices of LV function, including mean velocity of circumferential fiber shortening (Vcf) and shortening fraction (SF), have been variously reported to increase, remain constant or decrease during human pregnancy (Simmons et al., 2002; Mone et al., 1996; Kametas et al., 2001b). However, in mice pregnancy hypertrophy is associated with SF decrease, indicating a fall in systolic function (Eghbali et al., 2005). Thus, it is not clear whether gestational cardiac hypertrophy with improvement in systolic function occurs in all species.

In women mean arterial pressure diminishes during pregnancy reaching a nadir during mid gestation (Kametas et al., 2001a). This decrease in peripheral resistance is correlated with a fall in the resistance index (RI) of the uterine artery, which guarantees appropriate uterine blood flow for fetal development (Valensise et al., 2000; Mone et al., 1996).

Maternal cardiovascular maladaptation is highly correlated with adverse pregnancy outcomes (Easterling et al., 1987; Vasapollo et al., 2008). There is evidence that pregnancies complicated by intrauterine growth restriction are associated with impaired expansion of the maternal intravascular space and a lack of CO increase (Kametas et al., 2001a). Furthermore, increasing maternal arterial pressure produces pre-eclampsia, a hypertensive pregnancy disorder, where uterine artery RI and blood pressure increase, leading to abnormal fetal perfusion (Voss et al., 2006).

Studying maternal cardiovascular adaptation during pregnancy provides an insight into the interaction between maternal and fetal homeostasis and may prove a useful screening tool for pregnancy complications. There is limited information about cardiac function during normal gestation in dogs. In this species, LV end diastolic diameter (LVDd), end diastolic volume, LV free wall mass, stroke volume and CO have been shown to be elevated at days 50 and 60 of pregnancy (Williams et al., 2007). However, there is no information about these parameters throughout the complete gestation period, particularly in early and mid pregnancy. Reflex increase in heart rate (HR), plasma renin activity, concentrations of vasopressin, angiotensin- II, ACTH and cortisol have been shown to be attenuated during pregnancy (Brooks and Keil, 1994).

Blood pressure has been previously measured only on days 21–28, 40 and 60 of gestation in dogs (Lobo et al., 2009). Peripheral circulation has been described through uterine blood flow from the

* Corresponding author. Tel.: +54 221 423 6663; fax: +54 221 479 0544.
E-mail address: pgblanco@fcv.unlp.edu.ar (P.G. Blanco).

1090-0233/$ - see front matter © 2010 Elsevier Ltd. All rights reserved.
doi:10.1016/j.tvjl.2010.08.013

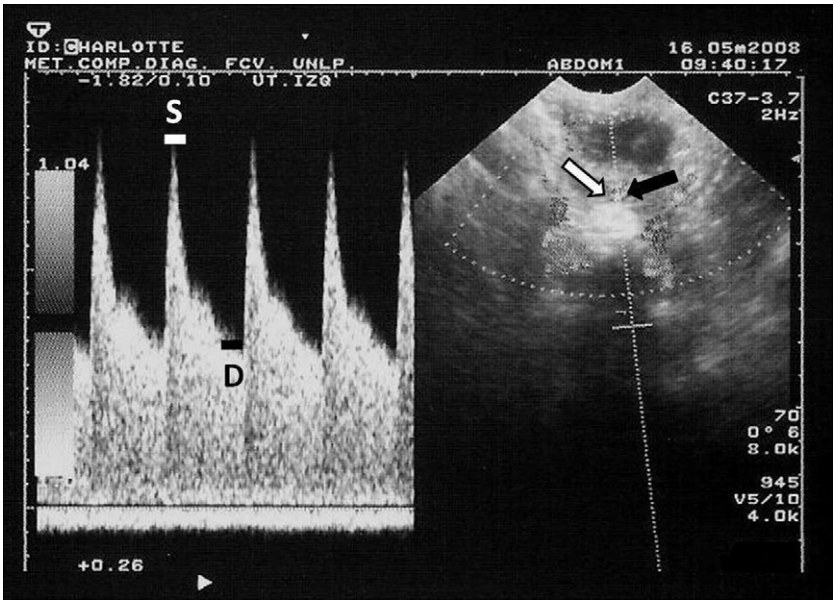

Fig. 1. Pulsed wave Doppler ultrasound register of uterine artery (white arrow) in a selected pregnant bitch 60 days after the estimated day of the luteinizing hormone peak. The cursor was positioned on the artery (black arrow). *S* is the peak systolic velocity and *D* the end diastolic velocity.

3rd and 4th week of normal gestation (Nautrup, 1998; Di Salvo et al., 2006) and during the 5th week in an experimental model of adverse pregnancy outcome (Blanco et al., 2009). However, uterine blood flow during the first 3 weeks of gestation is unknown. The aim of this study was to describe changes in cardiac morphology, systolic function and some peripheral hemodynamic parameters during normal canine pregnancy.

Materials and methods

Animals and follow up

This study was approved by the Faculty Institutional Care and Animal Use Committee (IACUC).

Twenty, 2.6 ± 1.2 (1–4) year-old, 12.9 ± 13.2 (3–38) kg, cross and pure-bred pregnant (PG; $n = 10$) and non-pregnant (CG; $n = 10$) healthy bitches were included in the study. Pregnancy was confirmed by ultrasound in all cases (England, 1998). The dogs were evaluated by ultrasound and echocardiography every 10 days from day 0 of the estrus cycle to parturition or to day 65 of the estrus cycle for the PG and CG, respectively. Day 0 of the estrus cycle was defined as the first day of typical estrus vaginal cytology (Olson et al., 1984).

Echocardiographic evaluations

M-mode, 2D and Doppler echocardiographic evaluations were carried out with the animals in standing position using a 7 MHz transducer (Toshiba Core Vision Pro; Chetboul et al., 2005). Acoustic gel was applied to the transducer and coupled directly to the clipped skin.

The right parasternal view was observed by locating the transducer between the right 3rd and 6th intercostal spaces between the sternum and costochondral junctions. Interventricular septum in diastole (IVSd; mm) and systole (IVSs; mm), LVDd (mm) and LV end systolic diameter (LVDs; mm), posterior wall in diastole (PWd; mm) and systole (PWs; mm) and SF (%) were detected in the short axis view, during M-mode tracing. To perform these measurements in the M-mode echocardiogram, a cross-sectional view of the LV was obtained at the level of chordae tendineae or the tips of the papillary muscles. The cursor was placed between these tips and then LV dimensions were measured as previously reported (Kienle, 1998). SF was calculated as $(LVDd - LVDs)/LVDd \times 100$ (Boon, 1998). Ventricular mass (VM; g), Vcf (circ/s), end systolic stress (ESS; dynes/cm^2) and index of relative wall thickness (RWT) were also calculated with the corresponding formula (Kienle, 1998; Boon, 1998; Vuille and Weyman, 1994).

In the right parasternal long axis view, left atrium to aorta ratio (LA/Ao), E-point to septal separation (EPSS; mm), aortic amplitude (AA; mm) and LV ejection time (LVET; ms) were recorded during M-mode tracing of mitral valve level and aortic valve level (Kienle, 1998). In the left parasternal window, the apical five chamber view was obtained. In all cases the cursor was aligned as parallel as possible to the aortic flow. Doppler gate was positioned just distal to the aortic valve. Stroke volume (SV; mL) was calculated as the product of the velocity time integral (VTI; measured by pulsed-wave Doppler) and the cross-sectional area of the aorta (Estrada and Maisenbacher, 2006). CO (L/min) was calculated as the product of SV and HR (bpm) derived from electrocardiographic monitoring. To minimize variability, three consecutive measurements of each parameter were recorded by a single trained operator following previous recommendations (Gottdiener et al., 2004). In case of marked sinus arrhythmia, six measurements of HR were performed.

Systolic blood pressure

Systolic blood pressure (SBP; mm Hg) was measured using a Doppler flow detector (DV610 Medmega). The cuff width was 40% of the circumference of the forelimb (Littman and Fox, 1999). Dogs were positioned in lateral recumbency and the assessment was carried out after 10 min of acclimatization. Then, three consecutive measurements were recorded from the same location and position.

Uterine blood flow assessment

RI of uterine artery was assessed by color and pulsed-wave Doppler ultrasound (Toshiba Core Vision Pro) with a 3.7–6 MHz convex transducer. Dogs were positioned in lateral recumbency. Color and pulsed-wave Doppler examinations were performed to obtain the waveforms as previously reported (Alvarez-Clau and Liste, 2005). The insonation angle was manually aligned and measurements with an angle > 20° were disregarded. RI is defined as $(S - D)/S$, where S is the peak systolic velocity and D the end diastolic velocity (Dickey, 1997). Three uniform consecutive waveforms were recorded to automatically calculate RI.

Statistical analysis

Normal distribution of the data was assessed and corroborated by Kolmogorov–Smirnov test. To verify the comparability of the groups, comparisons with regard to weight, age and breed were performed by the Kruskal–Wallis test for continuous variables and Fisher's exact test for categorical variables using GraphPad InStat software. The influence of these variables was also examined on cardiovascular variables by multivariate logistic regression analysis. IVDd, IVSs, LVDd, LVDs, PWd and PWs were normalized to bodyweight according to Cornell et al. (2004) and absolute changes of the Cornell index were calculated at each time point.

SF, VM, Vcf, ESS, RWT, LA/Ao, EPSS, AA, LVET, SV, CO, HR, SBP and RI were transformed to percentage change ([Final value - initial value / initial value] x 100). Comparisons between groups were carried out by repeated measures ANOVA followed by Tukey comparison test (SPSS 17.0; D'Amico et al., 2001).

Results

Original recordings of pulsed-wave Doppler ultrasound of uterine artery are shown in Fig. 1. Both groups of dogs were similar, considering weight, age and breed. Multivariate logistic regression

revealed that none of the analyzed variables significantly influenced the cardiovascular parameters ($P > 0.1$). At the beginning of the study, these parameters did not differ between groups ($P > 0.1$; Table 1). All the bitches presented values within the normal ranges for their weight (Cornell et al., 2004; Borgarelli et al., 2007; Schiller et al., 1983).

An interaction between time and group was found in changes in the Cornell index of PWs ($P < 0.05$; Table 2), percentage Vcf ($P < 0.01$; Fig. 2a), SF ($P < 0.01$; Fig. 2b), SV ($P < 0.05$; Fig. 2c), CO ($P < 0.01$; Fig. 2d) and HR ($P < 0.01$; Fig. 2e) changes throughout the study period. Velocity of circumferential fiber shortening and SF began to increase from day 30 onwards. Absolute changes in the Cornell index of PWs increased from day 50 up to day 60, while SV, CO and HR increased from day 40 onwards.

An interaction between time and group was found in percentage ESS ($P < 0.05$; Fig. 2f), SBP ($P < 0.05$; Fig. 3a) and RI ($P < 0.01$; Fig. 3b) changes during the same period. In PG bitches, ESS, SBP and RI decreased from day 30 to parturition. Absolute IVSd, IVSs, LVDs, LVDd and PWd changes in the Cornell index obtained from allometric scaling methods are shown in Table 2. Interventricular septum in diastole, IVSs, LVDd and LVDs significantly differed between PG and CG dogs, while percentage VM, RWT, LA/Ao, EPSS, AA and LVET changes did not (Table 3).

Table 1
Baseline cardiovascular parameters (mean ± SD) of 10 pregnant (PG) and 10 non-pregnant control (CG) female dogs. Cornell indices and ranges are shown for the M-mode parameters.

Parameter	PG	CG	Cornell ranges
Cornell index for IVSd (cm)	0.44 ± 0.04	0.46 ± 0.07	0.59–0.29
Cornell index for IVSs (cm)	0.58 ± 0.06	0.64 ± 0.08	0.43–0.79
Cornell index for LVDd (cm)	1.61 ± 0.18	1.65 ± 0.16	1.27–1.85
Cornell index for LVDs (cm)	1.03 ± 0.15	1.08 ± 0.15	0.71–1.26
Cornell index for PWd (cm)	0.37 ± 0.07	0.38 ± 0.06	0.29–0.60
Cornell index for PWs (cm)	0.60 ± 0.10	0.58 ± 0.09	0.48–0.87
SF (%)	32.4 ± 2.1	33.4 ± 3.2	
VM (g)	71.7 ± 82	70.6 ± 64	
Vcf (circ/s)	2.2 ± 0.7	2.0 ± 0.2	
ESS (dynes/cm^2)	74.2 ± 15	79.0 ± 21	
RWT	0.45 ± 0.1	0.40 ± 0.0	
LA/Ao	0.95 ± 0.0	0.92 ± 0.0	
ESSP (mm)	2.1 ± 0.5	2.8 ± 1.4	
AA (mm)	9.3 ± 3.3	9.8 ± 3.6	
LVET (ms)	177 ± 8	169 ± 9	
SV (mL)	24.0 ± 23	29.2 ± 20	
CO (L/min)	2.5 ± 2.3	2.8 ± 1.4	
HR (bpm)	122 ± 29	124 ± 22	
SBP (mm Hg)	140 ± 10	147 ± 11	
RI	0.86 ± 0.0	0.88 ± 0.0	

IVSd, interventricular septum in diastole; IVSs, interventricular septum in systole; LVDs, left ventricular end systolic diameter; LVDd, left ventricular end diastolic diameter; PWd, posterior wall in diastole; PWs, posterior wall in systole; SF, shortening fraction; VM, ventricular mass; Vcf, velocity of circumferential fiber shortening; ESS, end systolic stress; RWT, index of relative wall thickness; LA/Ao, left atrium to aorta ratio; EPSS, E-point to septal separation; AA, aortic amplitude; LVET, left ventricular ejection time; SV, stroke volume; CO, cardiac output; HR, heart rate; SBP, systolic blood pressure; RI, resistance index.

Discussion

Most of our results were in line with findings that have been described for humans, a species in which pregnancy is associated with increased maternal cardiac workload (Desai et al., 2004). In the present study, the increased thickening of cardiac walls indicates that, as in women (Kametas et al., 2001a), the heart develops hypertrophy during pregnancy in dogs, probably in response to volume overload (Williams et al., 2007). Furthermore, LVDd was higher in the PG dogs, which is consistent with previous reports of eccentric hypertrophy in other mammalians (Eghbali et al., 2005).

Hypertrophy is a physiological mechanism to maintain CO despite the chronically increased load on the LV. The most important stimulus for myocardial hypertrophy is the stretching of myocardial fibers (Eghbali et al., 2005). In mice, pregnancy cardiac hypertrophy can be distinguished from pathological hypertrophy by the lack of classical markers of pathological hypertrophy. In this species, physiological pregnancy hypertrophy is also associated with decreased expression of a pathological marker which can be down-regulated by estrogens (Eghbali et al., 2005). Some undetermined aspect of pregnancy, possibly hormonal, may be responsible for

Table 2
Absolute changes in Cornell index (cm) obtained from allometric scaling methods of 10 pregnant (PG) and 10 non-pregnant control (CG) female dogs assessed every 10 days during 2 months from estimated day of luteinizing hormone peak.

	Day of gestation					
	10	20	30	40	50	60
IVSd[a]						
PG	0.05 ± 0.03	0.04 ± 0.04	0.02 ± 0.04	0.01 ± 0.04	0.02 ± 0.04	0.01 ± 0.05
CG	0.00 ± 0.06	0.00 ± 0.05	0.00 ± 0.08	−0.05 ± 0.08	0.00 ± 0.08	−0.01 ± 0.08
IVSs[a]						
PG	0.04 ± 0.06	0.05 ± 0.06	0.04 ± 0.08	0.02 ± 0.06	0.06 ± 0.07	0.05 ± 0.08
CG	0.00 ± 0.09	−0.01 ± 0.07	0.00 ± 0.08	−0.05 ± 0.13	−0.00 ± 0.10	−0.03 ± 0.13
LVDd[a]						
PG	0.00 ± 0.13	−0.01 ± 0.14	0.00 ± 0.13	0.00 ± 0.13	−0.03 ± 0.10	0.00 ± 0.15
CG	−0.01 ± 0.11	−0.03 ± 0.11	−0.07 ± 0.09	−0.05 ± 0.10	−0.05 ± 0.10	−0.09 ± 0.16
LVDs[a]						
PG	−0.05 ± 0.08	−0.05 ± 0.09	−0.09 ± 0.16	−0.11 ± 0.12	−0.12 ± 0.10	−0.08 ± 0.11
CG	−0.03 ± 0.07	−0.03 ± 0.06	−0.04 ± 0.07	−0.02 ± 0.06	−0.01 ± 0.06	−0.02 ± 0.10
PWd						
PG	0.01 ± 0.04	−0.01 ± 0.07	−0.02 ± 0.06	0.00 ± 0.06	0.00 ± 0.08	0.00 ± 0.06
CG	0.03 ± 0.06	−0.02 ± 0.07	0.01 ± 0.07	−0.03 ± 0.07	0.00 ± 0.08	0.00 ± 0.08
PWs[b]						
PG	0.01 ± 0.06	0.00 ± 0.08	0.00 ± 0.09	0.03 ± 0.10	0.08 ± 0.10	0.04 ± 0.09
CG	0.05 ± 0.09	0.02 ± 0.13	0.03 ± 0.10	−0.01 ± 0.10	0.01 ± 0.09	0.03 ± 0.09

IVSd, interventricular septum in diastole; IVSs, interventricular septum in systole; LVDs, left ventricular end systolic diameter; LVDd, left ventricular end diastolic diameter; PWd, posterior wall in diastole; PWs, posterior wall in systole.
Superscripts represent significant ($P < 0.05$) differences between groups ([a]) or group by time interactions ([b]).

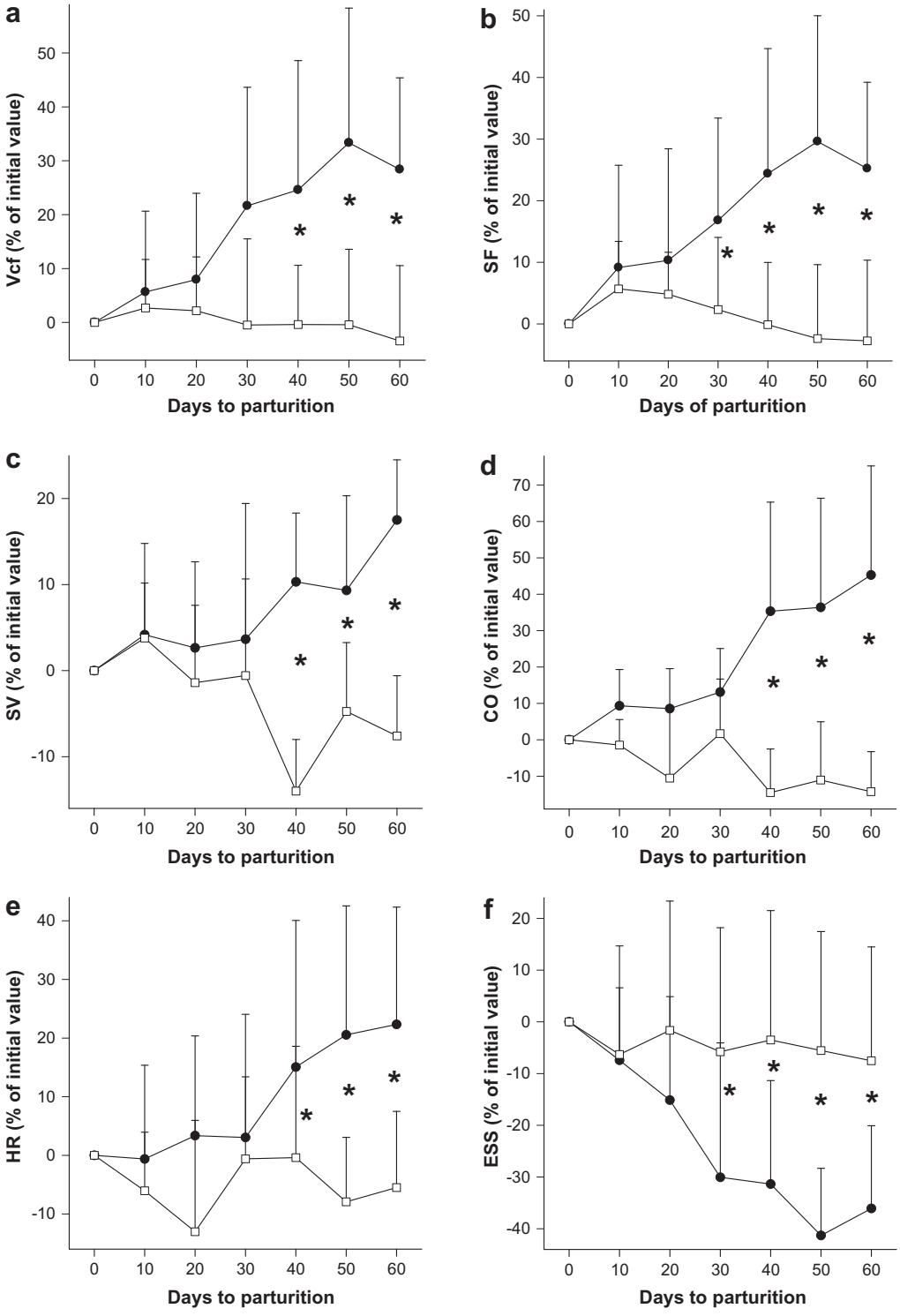

Fig. 2. Percentage cardiac parameters changes (mean ± SD) in pregnant (solid circles; $n = 10$) and non-pregnant (open squares; $n = 10$) bitches assessed every 10 days for 2 months. Day 0 was the estimated day of luteinizing hormone peak. (a) Percentage velocity of circumferential fiber shortening (Vcf) change. (b) Percentage shortening fraction (SF) change. (c) Percentage stroke volume (SV) change. (d) Percentage cardiac output (CO) change. (e) Percentage heart rate (HR) change. (f) Percentage end systolic stress (ESS) change. $^{*}p < 0.05$.

alterations in intrinsic myocardial properties independent of the associated hemodynamic changes (Mone et al., 1996). If this is correct, hormonal treatment may improve cardiac function in some cases of heart disease characterized by myocardial failure.

In contrast to women, where reports concerning Vcf and SF are contradictory (Simmons et al., 2002; Mone et al., 1996; Kametas et al., 2001b), these parameters were significantly higher in the PG dogs than in CG dogs from day 30 onwards. This finding also contrasted with prior work showing no change or a decrease in systolic function in late gestation in dogs (Williams et al., 2007; Lobo et al., 2009) and could be related to an improvement in systolic function most likely caused by the higher blood volume dur-

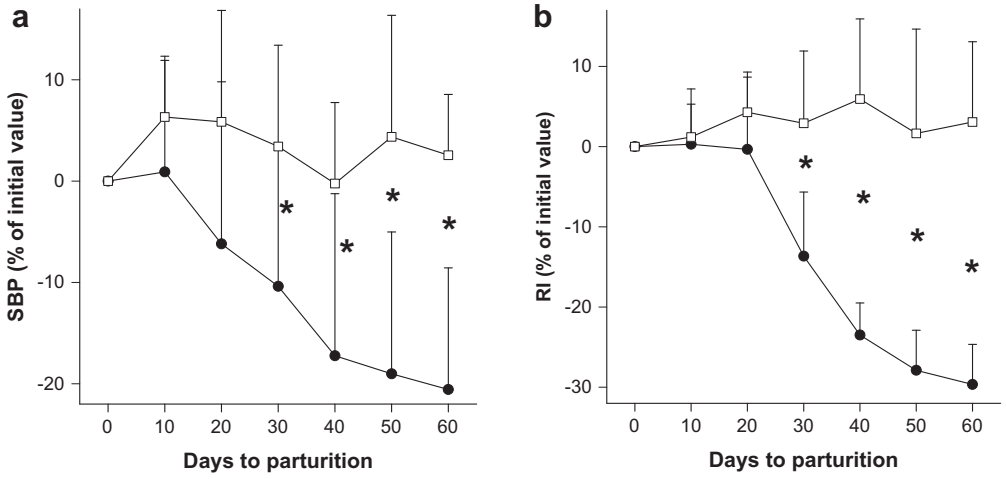

Fig. 3. Percentage peripheral hemodynamic parameters changes (mean ± SD) of the same animal groups and experiment of Fig. 2. (a) Percentage systolic blood pressure (SBP) change. (b) Percentage resistance index (RI) change. $^{*}p < 0.05$.

Table 3
Percentage echocardiographic parameter changes (mean ± SD) of 10 pregnant (PG) and 10 non-pregnant control (CG) female dogs assessed every 10 days over 2 months from the estimated day of the luteinizing hormone peak.

	Day of gestation					
	10	20	30	40	50	60
VM						
PG	6.5 ± 17	6.8 ± 17	3.1 ± 19	3.9 ± 14	11.7 ± 20	11 ± 27
CG	5.6 ± 21	−7.8 ± 18	−2.4 ± 24	−18.5 ± 17	−0.7 ± 29	−15 ± 35
RWT						
PG	−3 ± 7	−8.4 ± 32	−2 ± 21	4.8 ± 22	7.9 ± 21	−1.6 ± 27
CG	8.8 ± 22	−5.4 ± 21	10.9 ± 20	−5.4 ± 20	7.3 ± 24	11.7 ± 27
LA/Ao						
PG	−1.5 ± 16	0.5 ± 17	1.4 ± 14	5.8 ± 16	3.1 ± 12	−0.4 ± 17
CG	3.7 ± 6	3.4 ± 10	−0.9 ± 10	4.3 ± 6	−3 ± 8	2 ± 13
EPSS						
PG	8.9 ± 35	15 ± 50	3 ± 28	3 ± 40	3.5 ± 29	7.4 ± 41
CG	−6.3 ± 23	−7.6 ± 24	16.4 ± 20	−6.1 ± 29	−4.3 ± 25	−3 ± 28
AA						
PG	1.9 ± 9	5.5 ± 15	−2.3 ± 9	−6.3 ± 16	−4.2 ± 13	2.2 ± 17
CG	−2.2 ± 16	−4.6 ± 14	−1.3 ± 18	−7.2 ± 19	−3.8 ± 18	3 ± 19
LVET						
PG	3.6 ± 5	2.2 ± 8	4.3 ± 9	1.1 ± 8	−2.2 ± 8	−2.4 ± 10
CG	3.9 ± 7	2.4 ± 6	3.5 ± 10	0.1 ± 7	−2.13 ± 4	1.1 ± 7

VM, ventricular mass; RWT, index of relative wall thickness; LA/Ao, left atrium to aorta ratio; EPSS, E-point to septal separation; AA, aortic amplitude; LVET, left ventricular ejection time.

ing gestation and the increased wall dimensions. It is also possible that the increase in blood volume and a fall in systemic blood pressure influenced the changes in fractional shortening and systolic function. Considering the significant breed predisposition for myocardial disease (Kittleson, 1998), it would be interesting to evaluate whether systolic improvement varies among dog sizes. Unfortunately, in this study, we did not have enough large breeds to test this hypothesis.

The mechanisms resulting in increased arterial compliance include the augmentation of vascular distensibility and, possibly, the presence of the uteroplacental bed. As previously reported in dogs (Blanco et al., 2009; Nautrup, 1998; Di Salvo et al., 2006), the increasing density of fetal membranes and placental capillaries may induce a significant decrease in RI of the uterine artery. This reduction is associated with a decrease in total vascular resistance (Valensise et al., 2000), since both start to decrease from day 30 of pregnancy. It may also reflect hormonal influences on the peripheral circulation, such as the effects of increased nitric oxide availability in pregnancy (Simmons et al., 2002). Furthermore, the activity of the baroreceptor reflex in induced hypotension seems to be altered during canine pregnancy (Brooks and Keil, 1994). In contrast to a previous report in seven Saint-Bernard bitches, we found a decrease in this parameter. It would be interesting to test if this decrease is related to body size or breed and if it is also present in pathological gestations.

As afterload is reflected in peripheral resistance, a decrease in peripheral resistance is a major determinant of the augmentation of stroke volume and CO (Spotswood et al., 2006), which provides an appropriate blood flow to the conceptus. In this study, CO and stroke volume increased from day 40 of gestation, 10 days earlier than in previous reports (Williams et al., 2007). Increasing CO could also be due to the increased maternal HR, stroke volume and preload rise. Although anemia has been described during canine pregnancy (Concannon, 1983; Johnson, 2008), this would be insufficient to induce the modifications found in the maternal cardiovascular system.

Conclusions

Although the operator was not blind to the pregnancy status of the bitches, systolic cardiac function and peripheral circulation changed throughout the gestation period in dogs. A decrease in afterload, an increase in CO and cardiac hypertrophy appear to result from the hemodynamic modifications occurring during canine pregnancy. Therefore, in dogs, maternal cardiac adaptation during gestation plays a major role in uterine perfusion to support fetal development. The assessment of maternal cardiovascular function may prove a useful screening tool to detect pregnancy complications in dogs.

Conflict of interest statement

None of the authors of this paper has a financial or personal relationship with other people or organisations that could inappropriately influence or bias the content of the paper.

Acknowledgements

This study was partially funded by the University Incentive Program of Teaching & Research 11/V164. PGB and CG are Research Fellow and Career Scientist, respectively of National Research Council (CONICET) of Argentina.

References

Alvarez-Clau, A., Liste, F., 2005. Ultrasonographic characterization of the uterine artery in the nonestrus bitch. Ultrasound in Medicine and Biology 3, 1583–1587.

Blanco, P.G., Arias, D.O., Gobello, C., 2008. Doppler ultrasound in canine pregnancy. Journal of Ultrasound in Medicine 27, 1745–1750.

Blanco, P.G., Arias, D., Rube, A., Barrena, J.P., Corrada, Y., Gobello, C., 2009. An experimental model to study resistance index and systolic/diastolic ratio of uterine arteries in adverse canine pregnancy outcome. Reproduction in Domestic Animals 44, 164–166.

Boon, J., 1998. The echocardiographic examination. In: Boon, J.A. (Ed.), Manual of Veterinary Echocardiography. Williams and Wilkins, Media, pp. 35–128.

Borgarelli, M., Tarducci, A., Zanatta, R., Haggstrom, J., 2007. Decreased systolic function and inadequate hypertrophy in large and small breed dogs with chronic mitral valve insufficiency. Journal of Veterinary Internal Medicine 21, 61–67.

Brooks, V.L., Keil, L.C., 1994. Changes in the baroreflex during pregnancy in conscious dogs: heart rate and hormonal responses. Endocrinology 135, 1894–1901.

Chetboul, V., Tidholm, A., Nicolle, A., Sampedrano, C.C., Gouni, V., Pouchelon, J.L., Lefebvre, H.P., Concordet, D., 2005. Effects of animal position and number of repeated measurements on selected two-dimensional and M-mode echocardiographic variables in healthy dogs. Journal of the American Veterinary Medical Association 227, 743–747.

Concannon, P.W., 1983. Reproductive physiology and endocrinology patterns of the bitch. In: Kirk, R.W. (Ed.), Current Veterinary Therapy, vol. 1. W.B. Saunders Co., Philadelphia, pp. 886–901.

Cornell, C.C., Kittleson, M.D., Della Torre, P., Häggström, J., Lombard, C.W., Pedersen, H.D., Vollmar, A., Wey, A., 2004. Allometric scaling of M-mode cardiac measurements in normal adult dogs. Journal of Veterinary Internal Medicine 18, 311–321.

D'Amico, E.J., Neilands, T.B., Zambarano, R., 2001. Power analysis for multivariate and repeated measures designs: a flexible approach using the SPSS MANOVA procedure. Behavior Research Methods, Instruments and Computers 33, 479–484.

Desai, D., Moodley, J., Naidoo, D.P., 2004. Echocardiographic assessment of cardiovascular hemodynamics in normal pregnancy. Obstetrics and Gynecology 104, 20–29.

Di Salvo, P., Bocci, F., Polisca, A., 2006. Doppler evaluation of maternal and fetal vessels during normal gestation in the bitch. Research in Veterinary Science 81, 382–388.

Dickey, R.P., 1997. Doppler ultrasound investigation of uterine and ovarian blood flow in infertility and early pregnancy. Human Reproduction Update 3, 467–503.

Easterling, T.R., Watts, D.H., Schmucker, B.C., Benedetti, T.J., 1987. Measurement of cardiac output during pregnancy: validation of Doppler technique and clinical observations in preeclampsia. Obstetrics and Gynecology 69, 845–850.

Eghbali, M., Deva, R., Alioua, A., Minosyan, T.Y., Ruan, H., Wang, Y., Toro, L., Stefani, E., 2005. Molecular and functional signature of heart hypertrophy during pregnancy. Circulation Research 96, 1208–1216.

England, G.C.W., 1998. Ultrasonographic assessment of abnormal pregnancy. Ultrasonography 28, 849–867.

Estrada, A., Maisenbacher, H., 2006. Calculation of stenotic valve area. Journal of Veterinary Cardiology 8, 49–53.

Gottdiener, J.S., Bednarz, J., Devereux, R., Gardin, J., Klein, A., Manning, W.J., Morehead, A., Kitzman, D., Oh, J., Quinones, M., Schiller, N.B., Stein, J.H., Weissman, N.J., 2004. American Society of Echocardiography recommendations for use of echocardiography in clinical trials. Journal of the American Society of Echocardiography 17, 1086–1119.

Johnson, C.A., 2008. Pregnancy management in the bitch. Theriogenology 70, 1412–1417.

Kametas, N.A., McAuliffe, F., Hancock, J., Chambers, J., Nicolaides, K.H., 2001a. Maternal left ventricular mass and diastolic function during pregnancy. Ultrasound in Obstetrics and Gynecology 18, 460–466.

Kametas, N.A., McAuliffe, F., Cook, B., Nicolaides, K.H., Chambers, J., 2001b. Maternal left ventricular transverse and long-axis systolic function during pregnancy. Ultrasound in Obstetrics and Gynecology 18, 467–474.

Kienle, R.D., 1998. Echocardiography. In: Kittelson, M.D., Kienle, R.D. (Eds.), Small Animal Cardiovascular Medicine Textbook. Mosby, St. Louis, pp. 95–117.

Kittleson, M.D., 1998. Primary myocardial disease. In: Kittelson, M.D., Kienle, R.D. (Eds.), Small Animal Cardiovascular Medicine. Mosby, St. Louis, pp. 319–346.

Littman, M.P., Fox, P.R., 1999. Systemic hypertension: recognition and treatment. In: Fox, P., Sisson, D., Moïse, N.S. (Eds.), Textbook of Canine and Feline Cardiology. WB Saunders Co., Philadelphia, pp. 795–813.

Lobo, L., Salazar, L., Oliveira, P., Pereira, A., Fontes-Sousa, A.P., 2009. Echocardiographic evaluation of maternal cardiac function in the Saint Bernard dog. In: Proceedings of the 19th ECVIM-CA Congress, Porto, Portugal, pp. 1319–1350.

Mone, S.M., Sanders, S.P., Colan, S.D., 1996. Control mechanisms for physiological hypertrophy of pregnancy. Circulation 94, 667–672.

Nautrup, C.P., 1998. Doppler ultrasonography of canine maternal and fetal arteries during normal gestation. Journal of Reproduction and Fertility 112, 301–314.

Olson, P.N., Husted, P.W., Allen, T.A., Nett, T.M., 1984. Reproductive endocrinology and physiology of the bitch and queen. Veterinary Clinics of North America: Small Animal Practice 14, 927–946.

Schiller, N.B., Skiôldebrand, C.G., Schiller, E.J., Mavroudis, C.C., Silverman, N.H., Rahimtoola, S.H., Lipton, M.J., 1983. Canine left ventricular mass estimation by two-dimensional echocardiography. Circulation 68, 210–216.

Simmons, L., Gillin, A.G., Jeremy, R.W., 2002. Structural and functional changes in left ventricle during normotensive and preeclamptic pregnancy. American Journal of Physiology: Heart and Circulatory Physiology 283, H1627–H1633.

Spotswood, T.C., Kirberger, R.M., Koma, L.M., Thompson, P.N., Miller, D.B., 2006. Changes in echocardiographic variables of left ventricular size and function in a model of canine normovolemic anemia. Veterinary Radiology and Ultrasound 47, 358–365.

Valensise, H., Novelli, G.P., Vasapollo, B., Borzi, M., Arduini, D., Galante, A., Romanini, C., 2000. Maternal cardiac systolic and diastolic function: relationship with uteroplacental resistances. A Doppler and echocardiographic longitudinal study. Ultrasound Obstetrics and Gynecology 15, 487–497.

Vasapollo, B., Novelli, G.P., Valensise, H., 2008. Total vascular resistance and left ventricular morphology as screening tools for complications in pregnancy. Hypertension 51, 1020–1026.

Voss, A., Baumert, M., Baier, V., Stepan, H., Walther, T., Faber, R., 2006. Autonomic cardiovascular control in pregnancies with abnormal uterine perfusion. American Journal of Hypertension 19, 306–312.

Vuille, C., Weyman, A.E., 1994. Left ventricle I: general considerations, assessment of chamber size and function. In: Weyman, A.E. (Ed.), Principles and Practice of Echocardiography. Williams and Wilkins, pp. 575–624.

Williams, J.G., Rincon-Skinner, T., Sun, D., Wang, Z., Zhang, S., Zhang, X., Hintze, T.H., 2007. Role of nitric oxide in the coupling of myocardial oxygen consumption and coronary vascular dynamics during pregnancy in the dog. American Journal of Physiology: Heart and Circulatory Physiology 293, H2479–H2486.